Extraction of Kinetic Parameters for the Chemical Vapor Deposition of Polycrystalline Silicon at Medium and Low Pressures

Jisk Holleman and Jan F. Verweij

MESA Institute for Microelectronics, Materials Engineering and Sensors and Actuators, Faculty of Electrical Engineering, University of Twente, 7500 AE Enschede, The Netherlands

ABSTRACT

The deposition of silicon (Si) from silane (SiH_4) was studied in the silane pressure range from 0.5 to 100 Pa (0.005 to 1 mbar) and total pressure range from 10 to 1000 Pa using N_2 or He as carrier gases. The two reaction paths, namely, heterogeneous and homogeneous decomposition could be separated by varying the amount of wafer area per unit volume (wafer-distance variation) and the SiH_4 partial pressure as well as the total pressure. Rate constants were derived by fitting the experimental results. The heterogeneous reaction path could be described by only the adsorption rate constants of reactive species and the desorption rate constant of hydrogen using a Langmuir-Hinshelwood mechanism. Hydrogen and phosphine were found to suppress the deposition rate at low silane pressures. At high silane pressures or high total pressures the unimolecular decomposition of silane dominates. The unimolecular rate constant was found to be one to two orders larger than literature values based on RRKM analyses of high pressure rate data. The relative efficiency of SiH_4-N_2 and SiH_4-He collisions compared with SiH_4-SiH_4 collisions in the unimolecular gas-phase decomposition of SiH_4 has been investigated. Helium was found to be a weak collider compared to silane and nitrogen.

Polycrystalline silicon plays an important role in the semiconductor industry, namely, in integrated circuits (IC), thin film transistors (TFT), solar cells, and sensors. An extensive review of many scientific aspects and applications of polysilicon is given in Ref. 1.

In general polysilicon is deposited in hot-wall tube reactors where loads of 50 to 100 wafers are processed in one run. The depositions are performed using 100% SiH_4 or 23% SiH_4 diluted in an inert gas at SiH_4 partial pressures of between 10 and 30 Pa (0.1 to 0.3 mbar) at 625°C.[2,3] Under these conditions the growth rate is dominated by a Langmuir-Hinshelwood type of heterogeneous SiH_4 decomposition with H_2 release from Si-H bonds as the rate determining step.[4,5]

The unimolecular gas-phase decomposition becomes important at higher SiH_4 or higher total pressures. The homogeneous path is, in general, less desirable, because large polymers may be formed that coalesce to particles.[6] Thickness inhomogeneity at the wafer edge, due to local variation of the area per unit volume, is another problem related to highly reactive product formation in gas-phase reactions.[6-9]

However, in the case of *in situ* phosphorus or arsenic doping, the surface sites become blocked by PH_3- or AsH_3-related surface species, and the growth rate is strongly reduced.[7,10,11] In order to achieve reasonable growth rates the homogeneous path has then to be promoted thereby creating molecules and radicals that are more reactive than SiH_4 and are able to compete with PH_3 or AsH_3 for surface sites. The inhomogeneity at the wafer edge related to the gas-phase path and the discontinuity of area per unit volume at the wafer edge, the so called "bull's eye" effect, is caused by the high reactivity of the gas-phase products and can be solved by adjusting the quartz carrier design or by using cages.[12,13] In this way more area becomes available at the wafer edge to scavenge excess reactive gas-phase products. The gas-phase decomposition regime may also become important in single-wafer reactors where high throughputs are desired. If the total pressure is allowed to rise in single-wafer systems, a 2% nonpyrophoric dilution of SiH_4 related to its spontaneous flammability.[14]

The relative contributions of the different paths have been modeled in the past for both batch and single wafer reactors (see Ref. 15-20, and many other earlier references cited therein).

In this paper we report on a study of the decomposition of SiH_4 at low and medium pressures as well as the influence of the carrier and dopant gases.

Special attention is paid to the unimolecular gas-phase decomposition of SiH_4 into SiH_2, for which, in general, values were used, which up to now were derived by means of RRKM analyses[21-23] of experiments[24-26] at much higher pressure and/or lower temperature than generally applied in low pressure chemical vapor deposition (LPCVD) of polysilicon. In this paper values of the unimolecular rate constant and of the collision efficiency of the carrier gases He and N_2 are derived by making use of the effect that, due to the high reactivity of gas-phase reaction products, the growth rate becomes dependent on wafer spacing. We used this phenomenon for the separation of homogeneous and heterogeneous contributions to the total growth rate.

Experimental

Deposition.—The depositions were carried out on oxidized 3 in. wafers in a three-zone hot-wall horizontal tube reactor with 12 cm inner diameter. The length of the heating element is 90 cm with a flat temperature zone of 30 cm. The quartz wafer-carrier with slots at 5 mm spacing was positioned radially symmetrically in the reactor. The first and last five slot positions are always loaded with 3 in. wafers. In the experiments we varied the wafer spacing, gas flow rate, gas composition, and pressure. For the experiments presented in Fig. 2, 3, 4, 9, 10, and 11, the wafer spacing was varied alternatingly at 5 and 15 mm with the same run.

The experiments were performed in the temperature range from 525 to 700°C, this paper deals mainly with the experiments at 625°C. The temperature at the wafer-carrier position was calibrated by *in situ* thermocouple measurements and by using solid phase epitaxy of an amorphous layer, created by implantation of Si in monocrystalline silicon wafers, as a temperature monitor.[27] All experiments were performed with a so-called flat temperature profile at the carrier position. The wafer temperature was found to be independent of the pressure. With experiments at 500 Pa (5 mbar) we found that the temperature at the wafer position was no longer constant when the flow was larger than 1 slm. Therefore, the total flow was kept below 1 slm in the 500 and the 1000 Pa experiments.

All gases except SiH_4 had contamination levels below 1 ppm. The purity of SiH_4 was 99.995%.

Growth-rate measurements.—Growth rates were measured by weighing and by measuring the height of an etched step. The weighing method yields global growth rates whereas step-height measurements give information about the local growth rate and uniformity within the wafer. As a standard procedure the growth rates were measured at different positions in the wafer carrier, with various flow rates and various interwafer spacings.

In a horizontal hot-wall reactor, where Si wafers are placed in series with respect to the gas flow, the growth rate will decrease in the axial direction due to depletion of the reactant. The undepleted growth rate, r_o for high Péclet values can be determined by plotting the growth rate, r_x, at position x against the ratio A_x/MF according to Eq. 1 [28]

$$r = r_o[1 - \nu\{1 + (\epsilon - 1)(p_{SiH_4o}/p_{tot})\}A_x r_o MF^{-1}] \quad [1]$$

where A_x is the total hot surface area (wafers, wall, cantilever, carrier) upstream the position where r is measured, MF is the mass flow of SiH_4, ν is the overall order of the reaction, p_{SiH_4o} is the inlet partial pressure of SiH_4, p_{tot} is the total pressure, and ϵ is the number of gaseous molecules formed by the decomposition of one molecule of reactant.

Other authors ignored the hot surface area upstream the flat zone.[29,30] Although this area does not play a significant role in low depletion cases it cannot be ignored in most of the practical cases, and it is, in our opinion, the source of the lower activation energy of about 150 kJ mol^{-1} generally reported for LPCVD hot-wall silicon-deposition systems.[2,16,31-33] We found an apparent activation energy of 180 kJ · mol^{-1} in the temperature range 550-650°C, which is in agreement with values reported for single-wafer systems and molecular-beam reactors and in hot-wall reactors under conditions of low depletion.[5,30,34-38]

We determined the effective wall area upstream the flat zone by measuring the growth rate on silicon wafers placed close to the wall. The effective surface area of the entrance region was found to be 1200 cm^2.

The growth rates were also measured by varying the wafer spacing within the same run. When a surface reaction is the rate-determining step the growth rate is independent of the wafer spacing. However, when the gas-phase reaction leading to highly reactive components becomes important the growth rate will become a function of the density of surface area per unit volume. Gas-phase reactions have been reported for the deposition of silicon from SiH_4. [6,24,34,35,39-41]. These gas-phase reactions with SiH_2, Si_2H_6, Si_3H_8, and Si_2H_4 as major constituents contribute to the total deposition rate at higher pressures.

When gas-phase reactions become important, extrapolation according to Eq. 1 is no longer valid because the loss in the entrance region is now no longer determined by the effective wall area alone but also by the effective entrance volume. It is more convenient then to measure the loss in the entrance region for each run. The loss can be calculated by measuring the growth rate on silicon wafers placed horizontally close to the wall. The partial pressure of SiH_4 at the first wafer position can be calculated by equating the total flux, *i.e.*, convective and diffusion flux, at the first wafer position to the inlet flux minus the measured loss in the entrance region.

Results and Discussion

Growth rate.—The results of growth-rate measurements at various positions, flow rates, and wafer spacings are presented in Fig. 1 through 4. In Fig. 1 the wafer spacing was kept constant at 10 mm and the total pressure remained at 133 Pa using N_2 as a carrier gas. The undepleted growth rates, r_o, were obtained by extrapolation to the zero axis. In Fig. 2, 3, and 4 the wafer spacing was varied in order to separate surface and gas-phase decomposition of SiH_4. The undepleted total growth rates for 10 mm wafer spacing are presented in Fig. 5, along with results with the addition of PH_3. Also included in Fig. 5 are some data points (open circular markers) obtained previously in another reactor with N_2 and H_2 as carrier gases.[42] In Fig. 6 the uniformity

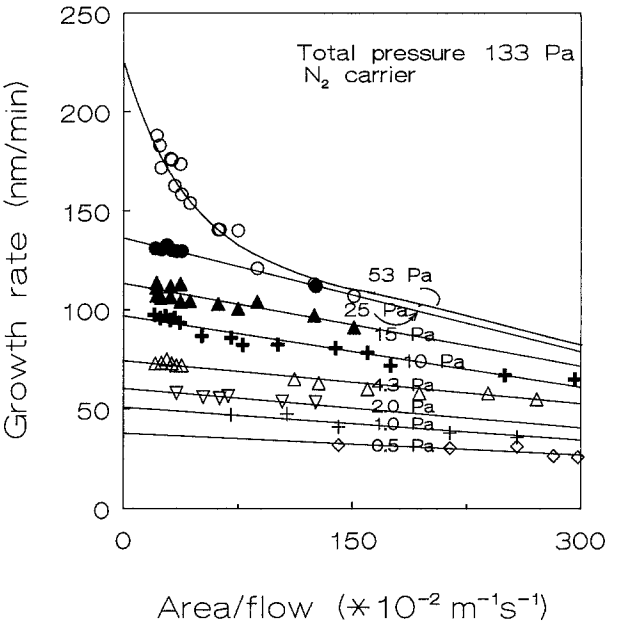

Fig. 1. Growth rate for various SiH_4 input partial pressures. Area/flow is the total growing surface area upstream of the position where growth is measured divided by the input flow of SiH_4. Total pressure is 133 Pa, carrier gas is nitrogen, wafer spacing is 10 mm, area per unit volume 159 m^{-1}. Deposition temperature is 625°C.

expressed as the ratio between the thickness at 2 mm from the wafer edge and the thickness in the center of the wafer is shown.

The Si growth, studied in the pressure range presented in Fig. 5, can be divided into three regions.

Region 1: SiH_4 partial pressures below 10 Pa. In this region the growth rate within the wafer is uniform, with edge/center ratios between 1 and 1.01, and independent of wafer spacing. The Si growth is moderately reduced by the addition of H_2 and strongly suppressed by PH_3.

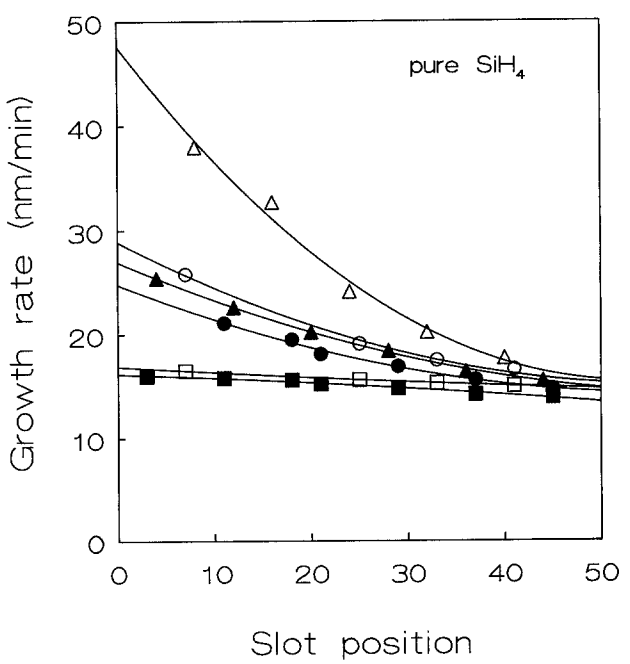

Fig. 2. Growth rate *vs.* slot position in the wafer carrier for various SiH_4 input pressures. Total pressure equals the SiH_4 input pressure. Slot spacing is 5 mm. Input is undiluted SiH_4. Wafer spacing: open markers 15 mm, filled markers 5 mm, area per unit volume 138 and 244 m^{-1}, respectively. SiH_4 flow is 88 sccm. Deposition temperature is 625°C. (△, ▲) p_{SiH_4} input 133 Pa; (○, ●) p_{SiH_4} input 80 Pa; (□, ■) p_{SiH_4} input 60 Pa.

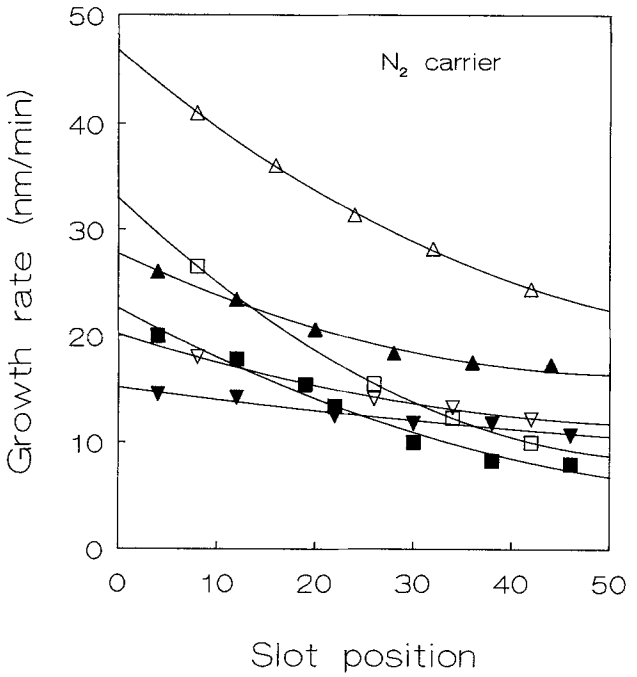

Fig. 3. Growth rate *vs.* slot position in the wafer carrier for various SiH_4 input partial pressures and total pressures. Slot spacing in carrier is 5 mm. Carrier gas is nitrogen. Wafer spacing: Open markers 15 mm, filled markers 5 mm, area per unit volume 138 and 244 m^{-1}, respectively. (△, ▲) total pressure 500 Pa, p_{SiH_4} = 40 Pa, SiH_4 flow = 62 sccm. (▽, ▼) total pressure 500 Pa, p_{SiH_4} = 25 Pa, SiH_4 flow = 44 sccm. (□, ■) total pressure 1000 Pa, p_{SiH_4} = 25 Pa, SiH_4 flow = 25 sccm. Deposition temperature is 625°C.

Region 2: SiH_4 partial pressures in the range of 10-35 Pa. In this region the growth rate is uniform for undoped polysilicon. The influence of H_2 for H_2-partial pressures in the range of 10-100 Pa is small to negligible, the suppression by PH_3 is moderate. The growth rate does not depend on wafer spacing in the case of undoped polysilicon layers whereas in the case of phosphorus-doped layers the growth rate is wafer spacing dependent. With the addition of PH_3 the uniformity decreases not only in a relative sense compared to undoped layers, but also the absolute difference between edge- and center-growth rate increases, indicating that the growth of polysilicon is not a simple addition of a heterogeneous and homogeneous contribution.

Region 3: SiH_4 partial pressures above 35 Pa. The growth becomes nonuniform, the edge/center growth-rate ratio increases. The growth rate is dependent on the partial pressure of the carrier gas but also depends on the wafer spac-

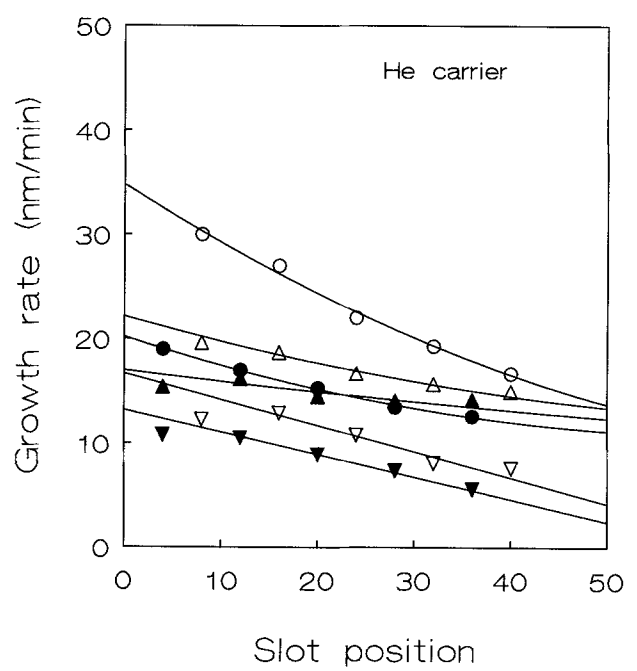

Fig. 4. Growth rate *vs.* slot position in the wafer carrier for various SiH_4 input partial pressures and total pressures. Slot spacing in carrier is 5 mm. Carrier gas is helium. Wafer spacing: Open markers 15 mm, filled markers 5 mm, area per unit volume 138 and 244 m^{-1}, respectively. (△, ▲) total pressure 500 Pa, p_{SiH_4} = 40 Pa, SiH_4 flow = 62 sccm; (○, ●) total pressure 1000 Pa, p_{SiH_4} = 40 Pa, SiH_4 flow = 40 sccm; (▽, ▼) total pressure 1000 Pa, p_{SiH_4} = 22 Pa, SiH_4 flow = 22 sccm. Deposition temperature is 625°C.

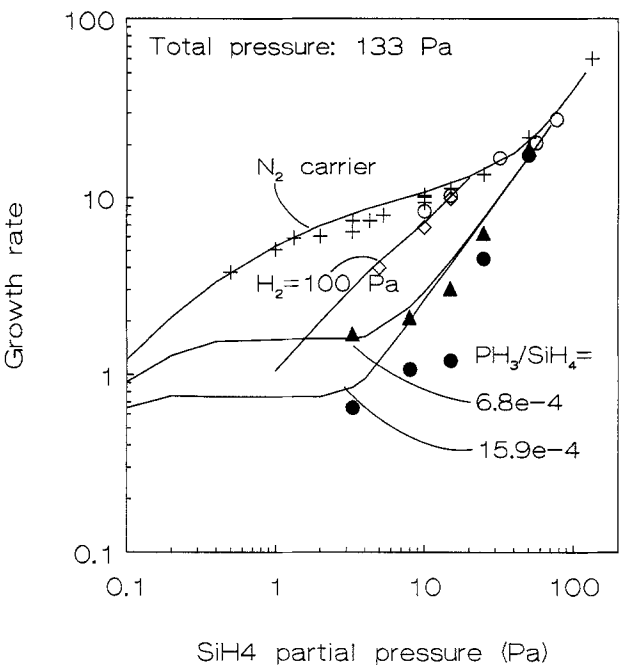

Fig. 5. Undepleted growth rate, wafer spacing is 10 mm, area per unit volume 159 m^{-1}. Deposition temperature is 625°C. Solid lines were calculated using parameters from Tables II and III.

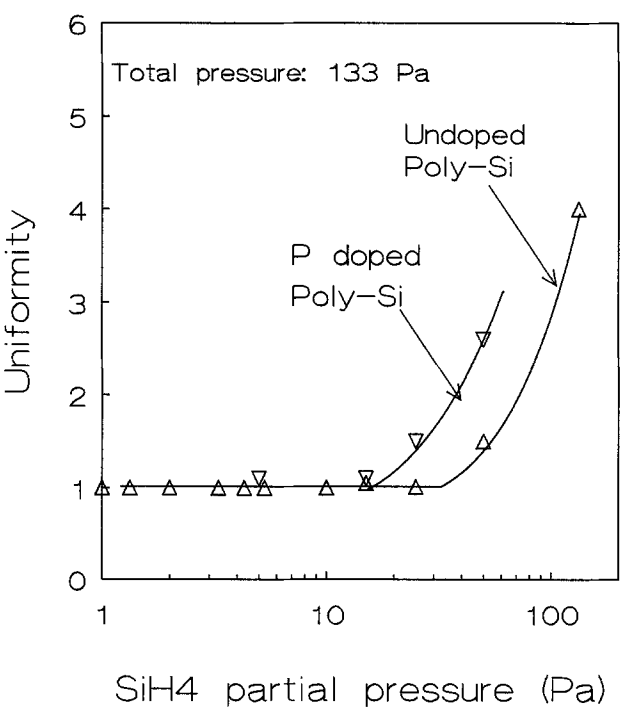

Fig. 6. Uniformity characterized by the ratio of growth rates at 1 mm from the edge and in the wafer's center.

ing. H_2 addition has no influence on growth rate. The suppression of growth due to PH_3 is small to negligible.

In order to study the effect of the carrier gas on the growth rate, experiments were carried out using N_2 and He as carrier gases up to pressures of 1000 Pa (10 mbar); see Fig. 3 and 4.

Heterogeneous surface decomposition.—In order to explain the observations in the three regions we propose considering the following sets of reactions

$$SiH_4 + (*)_2 \rightarrow SiH_3^* + H^* \quad \left(\underline{\underline{SiH_3\ H}}\right) \qquad [R\text{-}1]$$

$$SiH_3^* + * \rightarrow SiH_2^* + H^* \quad \left(\underline{\underline{SiH_2\ H\ H}}\right) \qquad [R\text{-}1a]$$

$$2SiH_2^* \rightarrow 2(Si)H^* + H_2 \quad \left(\underline{\underline{\overset{H}{\overset{|}{Si}}—\overset{H}{\overset{|}{Si}}}}\right) \qquad [R\text{-}1b]$$

$$2(Si)H^* \rightarrow 2Si + H_2 + 2^* \qquad [R\text{-}2a]$$

$$2H^* \rightarrow H_2 + 2^* \qquad [R\text{-}2b]$$

$(*)_2$ indicates a dual site, *i.e.*, two free sites at neighboring positions. The parentheses in (Si)H* indicate that the Si atom is bonded to the substrate with more than one bond and is therefore more or less immobile. There is no basic difference between (Si)H* and H* except that in (Si)H* the H* is bonded to the Si atom which originates from the gas-phase precursor. The exact sequence of decomposition is not known but from temperature-programmed desorption (TPD) measurements[4,5] and secondary ion mass spectroscopy (SIMS),[4] it appears that SiH_3^*, SiH_2, and SiH* are important intermediates in the surface decomposition of SiH_4. It is known from reaction freezing experiments followed by TPD or laser induced desorption (LID) that at normal polysilicon deposition conditions only the high temperature monohydride peak can be detected.[5] At large coverage the release of H_2 from (Si)H* and H* was found to be a process which is first order in H*,[4,5,43,44] which suggests a low mobility of the chemisorbed hydrogen atom.[45]

Our growth rate data in region 1 could be reasonably well described by a one-site chemisorption model using Kleijn's model parameters[15] with a correction of 20% for k_2. A dual-site chemisorption model, however, has been demonstrated to give a better fit over a larger pressure range.[18,46] Because we believe that dissociative chemisorption is more likely, in this paper the dual-site adsorption model is adopted to fit our growth rate data.

The surface decomposition for other silanes and silylenes, which are formed by gas-phase reactions as shown further on, is proposed to be similar to the surface decomposition of SiH_4.

The chemisorption reactions can be summarized as

$$Si_xH_y + (*)_a \rightarrow (Si_xH_y)^{a*} \qquad [R\text{-}3a]$$

$$(Si_xH_y)^{a*} + (y\text{-}z\text{-}a)^* \rightarrow x(Si)H^* + (y\text{-}z\text{-}x)H^* + z/2\ H_2 \qquad [R\text{-}3b]$$

where $(Si_xH_y)^{a*}$ indicates that Si_xH_y occupies a sites, either through dissociative adsorption, or by realizing a bonds per molecule, or by shielding of neighboring sites. Shielding becomes of importance when the chemisorbed species has a much larger diameter than the substrate atoms.

In the case of SiH_2, Si_2H_4, and Si_3H_8 formed due to gas-phase reactions, it has been suggested that the reactive sticking probability is high regardless of surface occupancy.[47] It has been demonstrated for Si_3H_8 [48] that it can adsorb in more than one monolayer, supporting the above assumption. It is known from gas-phase experiments that SiH_2 inserts with near unit probability in Si-H bonds in SiH_4, Si_2H_6, and Si_3H_8.[26,49] A similar insertion reaction to surface Si-H bonds is likely.

The following scheme is suggested for the reaction with occupied surface

$$Si_xH_y + H^* \rightarrow (HSi_xH_y)^* \qquad [R\text{-}4a]$$

$$(HSi_xH_y)^* \rightarrow H^* + x\ Si + y/2\ H_2 \qquad [R\text{-}4b]$$

$$(HSi_xH_y)^* + (*)_a \rightarrow H^* + (Si_xH_y)^{a*} \qquad [R\text{-}4c]$$

In words this means that the species adsorbed to occupied surface (R-4a) may either directly decompose (R-4b) without any interaction with surface sites or it may do so after interaction with free surface sites, R-4c, followed by R-3b. The suppression by PH_3 may be represented by the reaction

$$PH_3 + * \rightarrow PH_3^* \qquad [R\text{-}5a]$$

$$PH_3^* + 3^* \rightarrow P + 3H^* \qquad [R\text{-}5b]$$

The suppression of the surface reaction in region 1 by H_2, may proceed through reverse reactions like R-1b, R-2a, b, or R-3b and then through surface hopping H_2 may occupy surface sites, or interact directly with free surface sites.

The overall result is represented by

$$H_2 + (*)_2 \leftrightarrow 2H^*$$

It is of importance to note that Si_2H_6, SiH_2, Si_3H_8, PH_3 compete with SiH_4 for the same surface sites through the reactions R-3a, b, R-4c, and R-5a, b. Therefore, even if gas-phase products adsorb independently of occupancy, they may still interact in a subsequent step with free surface sites which would normally be available to SiH_4 chemisorption.

The essence of this competition is that the deposition of Si through the various reaction paths is not a simple addition of individual growth rates. Gradually when the gas-phase reactions become of more importance they will take over the role of SiH_4 due to their higher reaction probability. This effect leads to the conclusion that even if gas-phase reactions may already be significant they do not necessarily enhance the growth rate because of a simultaneous suppression of the SiH_4 surface decomposition. It is this effect that, in our opinion, determines the kinetics in region 2. The effect can be understood from Eq. 2 and 3 and is discussed in detail in the Section on Fitting of rate constants to experiments.

The gas-phase reactions, R-6, producing SiH_2, Si_2H_6, Si_2H_4, and Si_3H_8 are discussed in the Section on gas-phase reactions and collision efficiency.

The Langmuir-Hinshelwood growth rate equations.—The contribution to the deposition of Si by chemisorption reactions R-1a, R-3a and R-4a is given by

$$r = \sum_i x_i k_{i,*}[Si_{x_i}H_{y_i}](\theta_*)^{a_i} + x_i k_{i,H}[Si_{x_i}H_{y_i}](1 - \theta_*) \qquad [2]$$

where $k_{i,*}$ and $k_{i,H}$ are the adsorption rate constants on free and occupied surface sites, respectively, of species i, where species i is of the type Si_xH_y. It was assumed for SiH_4 and Si_2H_6 that $k_{i,H} = 0$, for SiH_2 and Si_3H_8 we assumed $k_{i,*} = k_{i,H}$, θ_* is the fraction of free surface sites, and a_i is the number of sites involved in the first step of chemisorption.

Equation 3 for the fraction of free surface sites θ_* can be derived by assuming that H* is the most abundant surface species and by assuming steady-state condition for H* · $dH^*/dt = \sum R_H = 0$, where R_H stands for all the H* and (Si)H* producing and destroying reactions and by setting * + H* = 1 we get * = 1/(1 + H*/*) which leads to

$$\theta_* = (1 + \sum n_i K_i [A_{x_i}H_{y_i}](\theta_*)^{(a_i - 1)})^{-1} \qquad [3]$$

$K_i = k_i/k_2$ with k_2 the desorption rate constant of H_2, n_i is the sum of H*, and (Si)H* formed during the total decomposition sequence of species i.

In $(A_{x_i}H_{y_i})$, A stands for either Si or P. In the particular case of H_2, A is no element which can be modeled by setting $x = 0$. For SiH_4 and Si_2H_6 we have set $n_i = (x_i + 2)$ which is for SiH_4 in agreement with the reaction sequence R-1 to R-2. Because SiH_2 and Si_3H_8 can adsorb and decompose

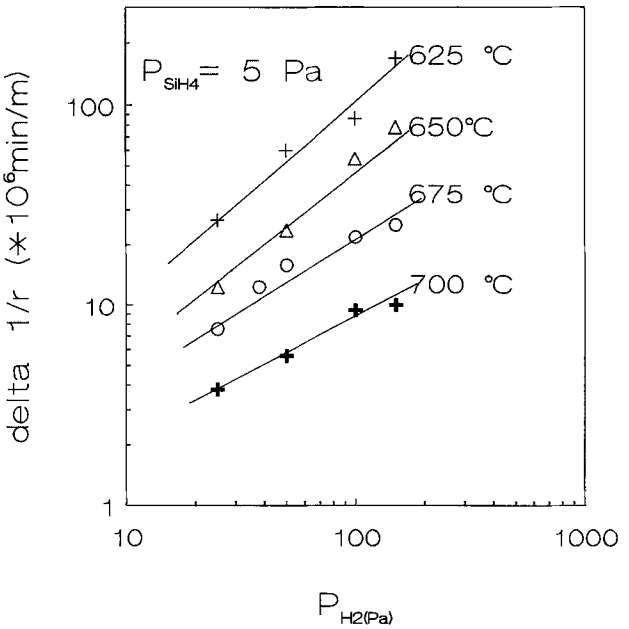

Fig. 7. Change in reciprocal growth rate at p_{SiH_4} = 5 Pa, the reference is at p_{H2} = 0.

along different paths, n_i for these species is somewhat more complicated. It was calculated for these two cases that

$$n_i = n_i'(1 + k_4b/k_4c)/(\theta_*^a + k_4b/k_4c) \quad [4]$$

with n_i' the number of H* sites formed along the path where surface sites are involved. Since the degree of suppression of heterogeneous decomposition of SiH_4 depends in particular on n_i of Si_3H_8, its value was fitted to the experimental results, see Table III and discussion thereafter.

At low pressures (region 1), it was found that the growth rate did not depend on wafer spacing. This can be explained, when it is assumed that the growth rate is dominated by r_{SiH_4}. At high pressures (region 3), however, a strong dependence is found on wafer spacing and the thickness uniformity was poor (see Fig. 6). Gas-phase reaction R-6 together with the amount of surface per unit volume determines the constrained steady-state concentrations of SiH_2, Si_2H_4, and Si_3H_8.

The silylene (SiH_2), formed by reaction R-6 has near-unit probability of reacting through insertion with other silanes.[26,49] Due to its high reactivity only SiH_2, formed in a thin sheet adjacent to the wafers, can reach the surface. In the bulk of the gas, SiH_2 transforms to Si_2H_6, Si_2H_4, and Si_3H_8. Other dimers and polymers may also be formed but were not considered in this paper. Apart from Si_2H_6 all reaction products have a high reactive sticking probability. Although the sticking probability of Si_2H_6 is higher than that of SiH_4, [46] it is still low enough not to be responsible for the edge nonuniformity. Even when the surface is already saturated with Si-H bonds, silylene (SiH_2), disilylene (Si_2H_4), trisilane (Si_3H_8), and higher polymers may be chemisorbed regardless of the occupation of surface sites. If such a mechanism is operating, the growth rate becomes dependent on the local density of surface which is generally discontinuous at the edge of the wafer causing the "bull's eye" effect.

Growth suppression by H_2.—In order to gain more insight into the role of H_2 in the deposition rate, we measured the growth rates at various partial pressures of H_2 and at various temperatures.

The change in the reciprocal growth rate $\Delta(r)^{-1}$ for $K_{H_2}[H_2]\theta_* < 1$, which is a reasonable assumption since the effect of H_2 on growth is small, can be derived from Eq. 2 and 3 and is given by

$$\Delta(r)^{-1} = 2K_{H_2}[H_2]/k_2K_1[SiH_4] \quad [5]$$

$\Delta(r)^{-1}$ was measured for $p SiH_4$ = 5 Pa and is shown in Fig. 7. The change in slope from 1 to 0.5 for increasing temperature is, in our opinion, related to the mobility of H* on the surface. Surface mobility is a thermally activated process and also dependent on the surface coverage, which generally increases with decreasing temperature. The desorption of H_2 from surface Si-H bonds at high coverage is a first-order process.[4,5,43,44] We think it may become a second-order process at higher temperatures and lower surface coverage due to increasing surface mobility.[45] This is in agreement with Schulze *et al.*[43] who attribute a symmetric TPD peak at low surface coverage to a second-order desorption process with a desorption energy of 240 kJ mol^{-1}. At high surface coverage they find the desorption to be first order with a desorption energy of 200 kJ mol^{-1}. An energy change of about 160 kJ mol^{-1} can be derived from the Arrhenius plot in Fig. 8 for the low temperature region where $\Delta(r^{-1})$ is linear with pH_2. For the poly-Si growth rate at very low surface coverage given by

$$r_{\theta_*=1} = k_1[SiH_4]$$

activation energies in the range of 0-30 kJ mol^{-1} have been reported.[4,5,35,37,46,50-52] Using this range the enthalpy change for H_2 chemisorption on a H* covered Si surface can then be calculated to be in the range from 160 to 190 kJ mol^{-1}. This is in agreement with ΔH values reported in the literature ranging from 150 to 200 kJ mol^{-1}. [53-55] Adopting the value of 195 kJ mol^{-1} for desorption of H_2 from a "Si-H" surface,[4,5,43,44] we calculated the barrier to chemisorption of H_2 to be in the range from 5 to 35 kJ mol^{-1}, which is in agreement with the 18 kJ mol^{-1} reported by Raff *et al.*[56] The barrier for the H_2 insertion reaction with SiH_2 is also reported to fall within this range.[26,34,57,58]

The reduction of growth due to H_2 has also been reported by Claassen *et al.* [30] and by Hottier *et al.*[51] Hottier also reports a first-order influence of H_2 at low temperature and a one-half order at high temperature.

Based on the calculations by Giling[53] one would also expect a substantial effect of H_2 under our experimental conditions. Others found no influence of H_2. [5,31,37,46] Those who reported no H_2 influence have either carried out their experiments in region 2, where we also measured no influence, or the amount of added H_2 was too small so that the effect was within experimental error. We think that the absence of H_2 effects in region 2 and 3 was due to the fact that the surface is too close to H* saturation Liehr[5] reported that H_2 adsorbs only slightly to Si, even at high

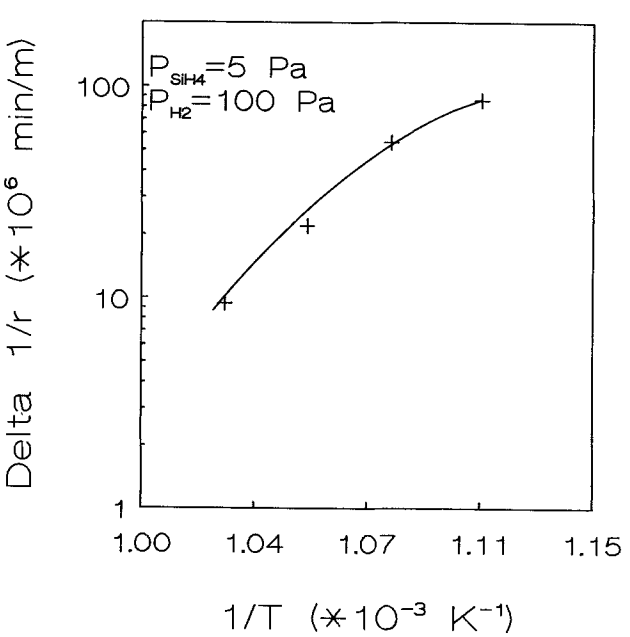

Fig. 8. Arrhenius plot of the change in reciprocal growth rate for p_{SiH_4} = 5 Pa and p_{H_2} = 100 Pa.

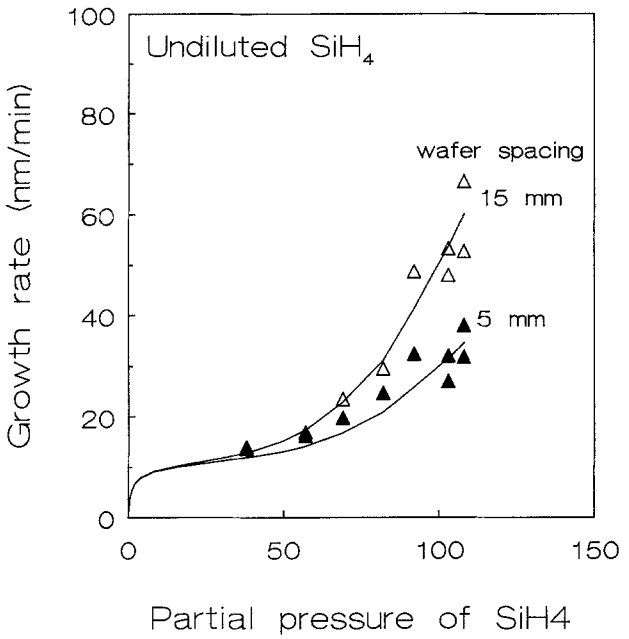

Fig. 9. Undepleted growth rate for 15 mm (open markers) and 5 mm (filled markers) wafer spacing, area per unit volume 138 and 244 m^{-1}, respectively. Input is undiluted SiH_4. Deposition temperature is 625°C. Solid lines were simulated using the parameters from Tables II and III.

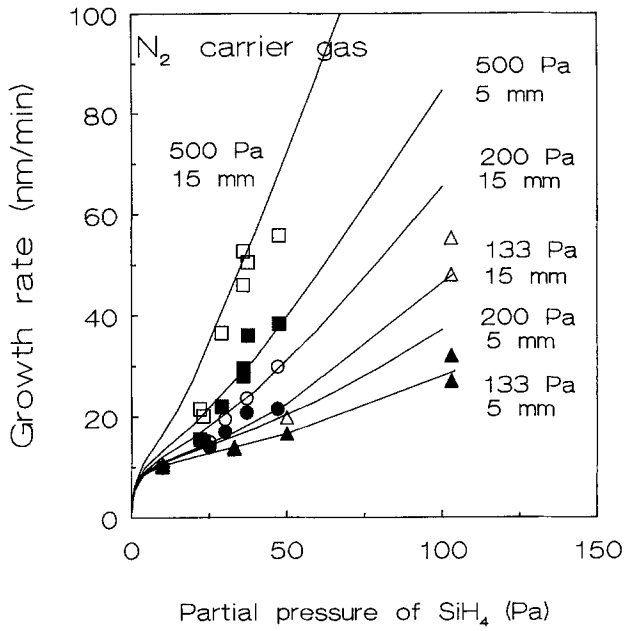

Fig. 10. Undepleted growth rate for 15 mm (open markers) and 5 mm (filled markers) wafer spacing. Area per unit volume is 138 and 244 m^{-1}, respectively. Carrier gas is N_2. Deposition temperature is 625°C. Solid lines were calculated with parameters from Tables II and III.

temperatures. The difference between Liehr's experiment and ours is that Liehr's experiments were performed on a clean Si surface whereas ours were performed on a H* covered surface. A lower barrier for H_2 chemisorption to a H* covered surface may explain the difference. The lower barrier reported for H_2 reaction with SiH_2 compared to a bare Si atom is indicative.[56-58]

In summary our conclusions at the end of this section are:

In region 1 growth is moderately suppressed by H_2.

Seemingly contradicting literature results on this topic are explained in terms of surface coverage.

Gas-phase reactions and collision efficiency.—Gas-phase reactions become important at higher SiH_4 pressures.[6,24,25,34,39-41] The unimolecular reaction R-6 proceeds through SiH_4-M collisional excitation, where M may be any gas-phase molecule, including SiH_4 itself

$$Si_xH_y \leftrightarrow Si_{x-1}H_{y-2} + SiH_2 \qquad [R\text{-}6]$$

Disilane, trisilane, and higher silanes are formed through insertion reactions of silylene with gas-phase silanes.

In our further discussion only SiH_2, Si_2H_6, and Si_3H_8 formation is taken into account because these are, besides SiH_4, the most abundant Si containing gas-phase species. Other reaction paths proposed by Coltrin *et al.*,[47] including higher silanes and silylenes, are now ignored, because any other path than the ones mentioned is controlled by the silylene formation in reaction R-6. Transport to the surface of silylene using higher silanes as an intermediate do not basically change the growth rate contribution along the homogeneous path.

In order to study the gas-phase reactions we have varied the total pressure and the partial pressure of SiH_4. The undepleted growth rates were derived in the manner presented in Fig. 2, 3, and 4. They are presented in Fig. 9 (pure SiH_4), Fig. 10 (N_2 carrier), and Fig. 11 (He carrier).

A considerable effect of wafer spacing on the growth rate is observed, indicating the homogeneous gas-phase formation of reactive species. The unimolecular decomposition of SiH_4 in the pressure range we have studied is, according to RRKM analyses,[21,22] in the low pressure limit regime, where the growth is dominated by the bimolecular reaction

$$SiH_4 + M \xrightarrow{k_c} SiH_4^a + M$$

where M can be any gas-phase molecule including SiH_4 itself. The subsequent decomposition of the energized SiH_4^a is given by

$$SiH_4^a \xrightarrow{k_a} SiH_4^+ \xrightarrow{k_+} SiH_2 + H_2$$

where SiH_4^+ is the activated complex. In the low pressure limit the basic equation for the decomposition rate constant is given by[59,60]

$$k_6 = \lambda Z(Q_2^*/Q_2)(p_{tot}/RT)\exp -E_o/RT \qquad [6]$$

Where Z is the collision number given by

$$Z = N_A\sigma^2_{SiH_4\text{-}M}[8\pi RT/M_{red}]^{1/2}\Omega^{2,2} \qquad [7]$$

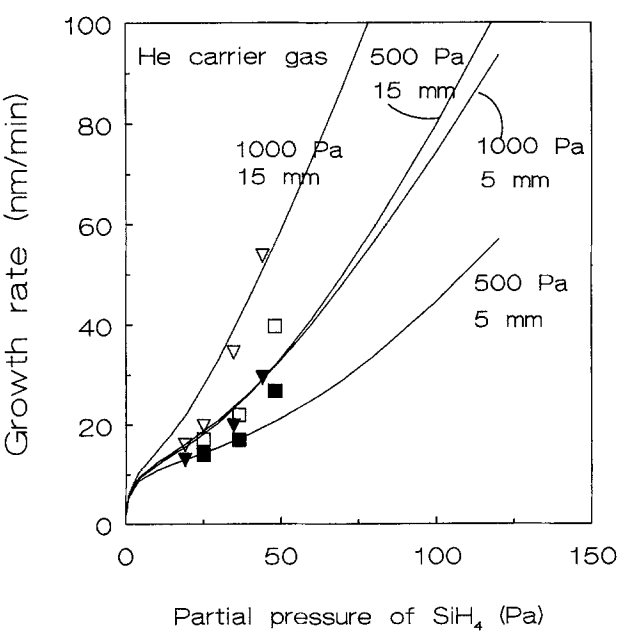

Fig. 11. Undepleted growth rate for 15 mm (open markers) and 5 mm (filled markers) wafer spacing. Area per unit volume 138 and 244 m^{-1}, respectively. Carrier gas is He. Deposition temperature is 625°C. Solid lines were calculated using parameters from Tables II and III.

Table I. Lennard-Jones collision parameters.

M	Mol. weight	σ(nm)	$\sigma_{SiH_4\text{-}M}$	M_{red}(kg/mol)	$\Omega^{2,2}$	$Z_{SiH_4\text{-}M}$
He	4	0.255	0.332	3.55E-3	0.73	3.54e8
N_2	28	0.397	0.403	14.96E-3	0.87	3.04e8
SiH_4	32, 12	0.408	0.408	22.71E-3	0.97	2.81e8

N_A is Avogadro's number, $\sigma_{SiH_4\text{-}M}$ is an effective collision diameter, and M_{red} is the reduced mass given by

$$M_{red} = M_{SiH_4}M_M/(M_{SiH_4} + M_M) \quad [8]$$

Q_2^* is the partition function of the activated complex using the ground state of SiH_4^* for the zero of energy. Q_2 is the partition function for the active degrees of freedom of the reactant SiH_4, λ is the collision efficiency, E_0 is the minimum energy required for decomposition.

In order to compare k_6 for different combinations we calculated the collision number for the various combinations. The approach proposed by Troe *et al.*[60] for the Lennard-Jones collision correction, $\Omega^{2,2}$, was used, see Table I.

In the case of a SiH_4-M mixture we can model the rate constant for gas-phase decomposition as

$$k = \sum_i k_i[M_i] \quad [13]$$

For those cases where λZ depends on M, the total pressure P_{tot} in Eq. 9 is replaced by

$$p_{eff} = p_{SiH_4} + \sum(\lambda_i' p_{M_i}) \quad [14]$$

where

$$\lambda' = \lambda\, Z_{SiH_4\text{-}M}/Z_{SiH_4\text{-}SiH_4} \quad [15]$$

It can be concluded from Fig. 9, 10, and 11 for the gas-phase contribution to the total growth rate that $k_{He\text{-}SiH_4} < k_{N_2\text{-}SiH_4} < k_{SiH_4\text{-}SiH_4}$. Since the collision number for He-SiH_4 is larger than for N_2-SiH_4 and SiH_4-SiH_4, the lower gas-phase contribution to the total growth rate has to be attributed to a lower collision energy transfer efficiency of He with SiH_4. The lower efficiency found for He in this work agrees with results in other works where He was shown to be one of the weaker colliders in unimolecular reactions.[61]

Conclusions of this section are:

In region 3 the growth is dominated by gas-phase reactions.

The growth rate results can be explained by SiH_4-M collisions where M may be any gas molecule including SiH_4 itself.

The collision efficiency of He in the gas-phase reaction is lower than that of SiH_4 and N_2.

Fitting of rate constants to experiments.—In order to calculate rate constants from our experimental results we adopted a few rate constants from the literature and present the values for T = 898 K and a total pressure of 100 Pa assuming $\lambda' = 1$, see Table II. The constants that were fitted to the experiments are summarized in Table III.

The reactive sticking coefficient of SiH_4 at zero coverage, $\gamma_{SiH_4,\theta_*=1}$, was fitted to the low pressure side of region 1 where it is most sensitive to it. The value is in good agreement with those reported by Kleijn (6e-4),[15] Gates (2-5e-4),[38] and Buss (1e-3).[46]

k_2 was fitted to the medium and high pressure side of region 1 which is insensitive to k_1.

K_{H_2} was fitted in region 1 where it is most significant. The effect of temperature on H_2 suppression of growth rate has already been discussed above. K_{PH_3} is very high and would correspond to an unrealistic reactive sticking coefficient of 2. However, qualitatively the high value agrees with 0.6 reported by Yu *et al.*[11] Our assumption that the Si_xH_y chemisorption on phosphorous sites is similar to chemisorption on silicon sites is possibly too much of a simplification. Also the adsorption and desorption reactions suggested in R-5 may be too simplified. No attempts were made in this paper to improve the model for PH_3 chemisorption. c and $n_{Si_3H_8}'$ are most significant in region 2. A value for $c << 1$ seems reasonable since the activation energy for surface hopping is much lower than for direct desorption.[45] The value for n is realistic because it means that nearly all H atoms in Si_3H_8 leave the surface as H_2 through H*. Also the low value for c indicates that the reaction path R-4b is negligible.

Region 3 is governed by k_{6,SiH_4} and the collision efficiencies. The rate constants adopted in Table II also determine the fitting of these parameters. Modification of the rate constants in Table II may change the relative contributions of SiH_2, Si_2H_6, and Si_3H_8. In extreme cases k_{6,SiH_4} for p_{eff} = 100 Pa may vary from 4.6e-1, if all gas-phase products deposit as SiH_2, to 2.3e-1 if all products deposit as Si_2H_6. The value for k_{6,SiH_4} which fits to our experiments is in good qualitative agreement with values found by Jeckel *et al.*[9] They reported values in the range of 5.6e-1 to 7.3e-1 s^{-1} for 100 Pa total pressure by fitting k_{6,SiH_4} to the experimentally found edge nonuniformity. If we calculate k_{6,SiH_4} from k_{-6} using Jasinsky's and Inoue's values[26,49] and thermochemistry,[15] we obtain 5.2e-1 using Jasinsky's value and 2.9e-1 using Inoue's value. These calculated values are also in good agreement with this work. A big disagreement is found with respect to RRKM analyses by Roenigk *et al.* (8.7e-3 at 100 Pa)[22] and Meyerson *et al.* (4.3e-3 at 100 Pa).[21]

The low efficiency for He is typical for this element[61] but was not confirmed by Jasinsky's[26] room-temperature measurement. Moffat's RRKM analyses[23] show no He influence for their best fit but with a slight modification of the assumptions they demonstrate that the RRKM analysis can predict a considerable lower efficiency for He.

Using the rate constants in Tables II and III, we calculated the growth rates and these are presented as solid lines in Fig. 5, 9, 10, 11, and 12. In Fig. 12 the calculated individual contributions to the growth rate of SiH_4, Si_2H_6, and Si_3H_8 are presented. The suppression of the SiH_4 contribution by higher silanes is clearly demonstrated in Fig. 12.

Table II. Kinetic parameters obtained from the literature

Constant	Value at 898 K and 100 Pa total pressure	Remarks
k_{3,Si_2H_6}	5.5 m s^{-1}	Adsorption rate constants were calculated using $k_{3,Si_xH_y} = 1/4\gamma_{Si_xH_y}\langle v\rangle$ with $\gamma_{Si_2H_6}$ = 4 e-2 [Ref. 4, 46].
k_{3,SiH_2}	199 m s^{-1}	
k_{3,Si_3H_8}	119 m s^{-1}	γ_{SiH_4,Si_3H_8} = 1, see text.
k_{6,Si_2H_6}	7.8e2 s^{-1}	Calculated from k_{-6} using thermochemistry calculations by Kleijn.[15]
k_{6,Si_3H_8}	5.5e2 s^{-1}	
k_{-6,SiH_4}	1e5 m^3/mol s	Calculated from room temperature measurements by Jasinsky *et al.*[26] assuming E_a = 0 and k_{-6} is proportional to $T^{0.5}$ and the order in total pressure 1 for SiH_4 and 0.5 for Si_2H_6 and Si_3H_8.[22,26]
k_{-6,Si_2H_6}	5.2e7 m^3/mol s	
k_{-6,Si_3H_8}	1.2e8 m/mol s	

Table III. Kinetic parameters obtained by fitting of measurements.

Constant	Value at 898 K and 100 Pa total pressure	Remarks
$\gamma_{SiH_4,\theta_*=1}$	8e-4 (±15%)	Reactive sticking coeff. at zero surface coverage.
k_1	1.54e-1 (±15%) m s^{-1}	$^{1/4}\gamma_{SiH_4,\theta_*=1} \langle v_{SiH_4} \rangle$
k_2	5.2e-5 (±6%) mol m^{-2} s^{-1}	H_2 desorption rate constant, see R-2.
E_a	180 kJ mol^{-1} (±5%)	Apparent overall activation energy in the temperature range 550 to 650°C.
E_{a,k_2}	195 kJ mol^{-1} (±5%)	Calculated activation energy for H_2 desorption assuming E_{a,k_1} = 15 kJ mol^{-1}.
K_{H_2}	470 m^3 mol^{-1} (±15%)	Equilibrium constant for H_2 adsorption, See Eq. 3.
ΔH_{H_2}	160-190 kJ mol^{-1}	Enthalpy change for H_2 chemisorption.
K_{PH_3}	7e-6 m^3 mol^{-1}	Steady-state constant for PH_3 adsorption, see Eq. 3.
k_{6,SiH_4}	3.5e-1 (±10%) s^{-1}	Unimolecular rate constant for SiH_4, see R-6. Linear in p_{tot} [21,22,26]
c	0.05 (±0.05)	Ratio k_4b/k_4c.
$n'_{Si_2H_6}$	7.5 (±1)	See Eq. 4.
$\lambda'N_2$	0.8 (±15%)	See Eq. 6 and 15.
$\lambda'He$	0.3 (±15%)	See Eq. 6 and 15.

The fits to Fig. 10 and Fig. 11 could be improved if we assume the effective total pressure as $p_{eff} = (1 + \alpha)p_{SiH_4} + (p_{tot} - p_{SiH_4})\lambda$. The physical interpretation of the fitting parameter α would be that other reaction paths independent of the total pressure exist, *e.g.*, SiH_4-SiH_4 collisions directly leading to reactive products like, *e.g.*, Si_2H_6 or Si_2H_4.

Conclusions

The growth rate of polysilicon at LPCVD conditions can be modeled by contributions of heterogeneous and homogeneous decomposition reactions.

At low pressures where the contribution by the homogeneous gas-phase reaction is negligible the growth rate is suppressed by H_2 and strongly suppressed by PH_3. At higher pressures the contribution by SiH_4 is also suppressed by reactive products formed due to gas-phase reactions such as SiH_2 and Si_3H_8.

The heterogeneous decomposition of Si_xH_y can be described by only two rate constants, namely, the adsorption rate constant of Si_xH_y and the desorption rate constant of H_2.

Many reaction parameters can be used to fit the experimental results but by adopting independently achieved constants from the literature, the number of parameters to be fitted can be kept to a minimum.

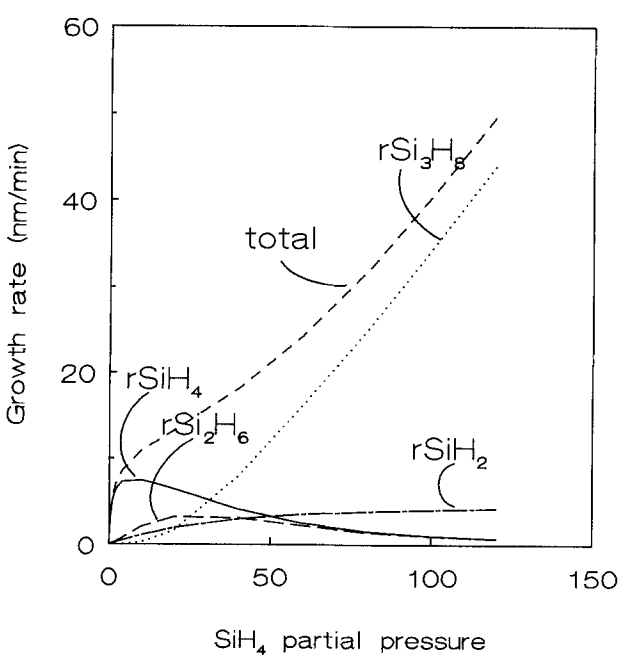

Fig. 12. Calculated contribution to the total growth rate at 625°C by SiH_4, SiH_2, Si_2H_6, and Si_3H_8 for 10 mm wafer spacing. Total pressure was 133 Pa in N_2 carrier gas.

The gas-phase decomposition reaction $SiH_4 \rightarrow SiH_2 + H_2$ has a much higher rate constant than was obtained from RRKM analyses.

The collision efficiency of He in gas-phase reactions is lower than the collision efficiency of N_2 and SiH_4.

Kinetic parameters have been extracted which enable us to predict the total growth rate for a wide range of pressure conditions, carrier gases, dopants, and loadings.

Acknowledgments

The authors would like to thank Dr. I. Barsony and J. Baxter for carefully reading the manuscript and for their help with the English language. Dr. J. G. E. Gardeniers for the valuable discussions on the chemistry and J. A. A. Stegeman for performing the experiments that led to this paper.

Manuscript submitted Nov. 5, 1992; revised manuscript received March 31, 1993.

The University of Twente assisted in meeting the publication costs of this article.

REFERENCES

1. T. I. Kamins, in *Polycrystalline Silicon for Integrated Circuit Applications,* Kluwer Academic Publishers, Amsterdam (1988).
2. R. S. Rosler, *Solid State Technol.*, **20,** 63 (1977).
3. W. A. Brown and T. I. Kamins, *ibid.*, **22,** 51 (1979).
4. S. M. Gates *et al., J. Vac. Sci. Technol. A,* **8**(3), 2965 (1990).
5. M. Liehr *et al., Appl. Phys. Lett.*, **56,** 629 (1990); M. Liehr *et al., J. Vac. Sci. Technol. A,* **8**(3), 2960 (1990).
6. C. H. J. van den Brekel and L. J. M. Bollen, *J. Crystal Growth,* **54,** 310 (1981).
7. B. S. Meyerson and W. Olbricht, *This Journal,* **131,** 2361 (1984).
8. A. Yeckel and S. Middleman, *ibid.*, **134,** 1279 (1987).
9. A. Yeckel and S. Middleman, *ibid.*, **136,** 2038 (1989).
10. M. L. Hitchman and W. Ahmed, *Vacuum,* **34,** 979 (1984).
11. M. L. Yu and B. S. Meyerson, *J. Vac. Sci. Technol. A,* **2,** 446 (1984).
12. J. G. M. Mulder, P. Eppenga, M. Hendriks, and J. E. Tong, *This Journal,* **137,** 273 (1990).
13. C. Azzaro, P. Duverneuil, and J. P. Couderc, *J. de Physique IV,* **C2,** 71 (1991).
14. L. G. Britton and P. Taylor, *Semiconduct. Int.*, 88 (April 1991).
15. C. R. Kleijn, *This Journal,* **138,** 2190 (1991).
16. G. Peev *et al., Semicond. Sci. Technol.*, **6,** 281 (1991).
17. T. A. Badgwell, T. F. Edgar, and I. Trachtenberg, *This Journal,* **139,** 524 (1992).
18. W. G. Houf, J. F. Grcar, and W. G. Breiland, Paper presented at E-MRS Spring Meeting, Strassbourg, France, June 2-5, 1992.
19. C. Azzaro, P. Duverneuil, and P. Couderc, *This Journal,* **139,** 305 (1992).
20. P. Duverneuil and J. P. Couderc, *ibid.*, **139,** 296 (1992).

21. B. S. Meyerson and J. M. Jasinski, *J. Appl. Phys.*, **61,** 785 (1987).
22. K. F. Roenigk, K. F. Jensen, and R. W. Carr, *J. Phys. Chem.*, **91,** 5732 (1987).
23. H. K. Moffat, K. F. Jensen, and R. W. Carr, *ibid.*, **95,** 145 (1991).
24. J. H. Purnell and R. Walsh, *Proc. R. Soc. London, Ser. A,* **293,** 543 (1966).
25. C. G. Newman, H. E. O'Neal, M. A. Ring, F. Leska, and N. Shipley, *Int. J. Chem. Kinet.*, **11,** 1168 (1979).
26. J. M. Jasinski and J. O. Chu, *J. Chem. Phys.*, **88,** 1678 (1988).
27. G. L. Olson and J. A. Roth, in *Kinetics of Solid Phase Crystallization in Amorphous Silicon,* North-Holland, Amsterdam (1988).
28. J. Holleman and J. Middelhoek, *Thin Solid Films,* **114,** 295 (1984).
29. A. E. T. Kuiper, C. J. van Den, J. de Groot, G. W. Veltkamp, *This Journal,* **129,** 2288 (1982).
30. W. A. P. Claassen *et al.*, *J. Crystal Growth,* **57,** 259 (1982).
31. W. Foster, A. J. Learn, and T. I. Kamins, *J. Vac. Sci. Technol. B,* **4,** 1182 (1986).
32. B. S. Meyerson, B. A. Scott, and R. Tsui, *Chemtronic,* **1,** 150 (1986).
33. B. A. Scott, R. D. Estes, and J. M. Jasinski, *J. Chem. Phys.*, **89,** 2544 (1988).
34. R. T. White, *et al.*, *J. Chem. Kinetic.*, **17,** 1029 (1985).
35. T. J. Donahue and R. Reif, *This Journal,* **133,** 1691 (1986).
36. J. J. J. Hajjar, R. Reif, and D. Adler, *J. Electronic Mater.*, **15,** 279 (1986).
37. J. Comfort and R. Reif, *This Journal,* **136,** 8 (1989).
38. S. M. Gates and S. K. Kulkarni, *Appl. Phys. Lett.*, **58,** 2963 (1991).
39. T. R. Hogness, T. L. Wilson, and W. Johnson, *J. Am. Chem. Soc.*, **58,** 108 (1936).
40. B. A. Scott, R. M. Plecenik, and E. E. Simonyi, *Appl. Phys. Lett.*, **39,** 73 (1981).
41. B. A. Scott *et al.*, *J. Vac. Sci. Technol. A,* **2,** 450 (1984).
42. J. Holleman and A. A. I. Aarnink, in *Chemical Vapor Deposition, 1981,* J. M. Blocher, Jr., G. E. Vuillard, and G. Wahl, Editors, PV 81-7, p. 307, The Electrochemical Society Softbound Proceedings Pennington, NJ (1981).
43. G. Schulze and M. Henzler, *Surf. Sci.*, **124,** 336 (1983).
44. K. Sinniah *et al.*, *Phys. Rev. Lett.*, **62,** 567 (1989).
45. F. C. Tompkins, in *Chemisorption of Gases on Metals,* Academic Press, Inc., London (1978).
46. R. J. Buss *et al.*, *J. Appl. Phys.*, **63,** 2808 (1988).
47. M. E. Coltrin, R. J. Kee, and G. H. Evans, *This Journal,* **136,** 819 (1989).
48. S. M. Gates, *Surf. Sci.*, **195,** 307 (1988).
49. G. Inoue and M. Suzuki, *Chem. Phys. Lett.*, **122,** 361 (1985).
50. R. F. C. Farrow, *This Journal,* **121,** 899 (1974).
51. F. Hottier and R. Cadoret, *J. Crystal Growth,* **52,** 199 (1981).
52. D. J. Robins and I. M. Young, *Appl. Phys. Lett.*, **50,** 1575 (1987).
53. L. J. Giling, H. H. C. de Moor, P. J. H. Jacobs, and A. A. Saaman, *J. Crystal Growth,* **78,** 303 (1986).
54. J. G. E. Gardeniers, M. M. W. Mooren, M. H. J. M. de Croon, and L. J. Giling, *ibid.*, **102,** 233 (1990); J. G. E. Gardeniers, L. J. Giling, F. de Jong, and J. P. van der Eerden, *ibid.*, **104,** 727 (1990).
55. P. Gupta, V. L. Colvin, and S. M. George, *Phys. Rev. B,* **37,** 8234 (1988).
56. L. M. Raff, I. NoorBatcha, and D. L. Thompson, *J. Chem. Phys.*, **85,** 3081 (1986).
57. M. S. Gordon, *J. Chem. Soc. Chem. Commun.*, 890 (1981).
58. R. S. Grev and H. F. Schaefer, *ibid.*, 785 (1983).
59. R. J. Robinson and K. A. Holbroek, in *Unimolecular Reactions,* John Wiley & Sons, Ltd., London (1972).
60. J. Troe, *J. Chem. Phys.*, **66,** 4758 (1977).
61. Y. N. Lin and B. S. Rabinovitch, *J. Phys. Chem.*, **72,** 1726 (1968).

Electrochemical Detection of Defects in Ge/GaAs Structures by an Anodic Dissolution Method under Illumination

Koichi Matsushita, Ryou Chiba, Sumio Okuyama, and Yasuji Kumagai

Department of Electrical and Information Engineering, Faculty of Engineering, Yamagata University, Yonezawa 992, Japan

ABSTRACT

Detection of crystal defects in Ge/GaAs structure has been studied by an electrochemical etching under illumination. Germanium film grown by the plasma-assisted epitaxy method with hydrogen on a semi-insulating GaAs substrate is anodically dissolved in a NaOH solution. Hillocks connected with the structural defect are then detected and their densities are estimated. Results obtained suggest that the defects in the Ge film originate from plasma ion bombardment, related to those in the GaAs substrate.

Semiconductor crystalline films with heterostructure have been recently made by several different epitaxial growth methods. Detection of crystal defects in such films is very important and particularly necessary for the characterization of the film used in optoelectronic devices.[1] For bulk semiconductor material, chemical etching is one of the most convenient techniques available for the detection. However, for films with a thickness less than 1 μm, the conventional chemical etching method cannot be used because of high etching rates.[2]

Yamamoto *et al.* have reported an electrochemical etching method in which the surface of n-type GaAs and InP is anodically dissolved under illumination and crystal defects are detected as etch hillocks.[3,4] The hillock formation results from decreases in the dissolution rate of the surface under which defects are located because of rapid recombination of holes. Etched depth in this case is less than 1 μm.

The purpose of this paper is to present results concerning crystal defects of an epitaxially grown germanium film and its substrate.

In connection with our study of low temperature epitaxial film growth technology, we formed epitaxially Ge films on GaAs using a hydrogen plasma sustained by radio frequency (RF) excitation and detected the crystal defects of the film and the GaAs substrate, using the above-mentioned etching method.[5,6] To obtain additional data, defects of Ge wafers were investigated in the same way as stated above.

Experimental

The sample holder and the apparatus used for anodic dissolution of Ge and GaAs are schematically illustrated in Fig. 1a and b, respectively.

The electrolyte used here was an NaOH solution with the concentration of 1 mol/liter at room temperature. The sample holder was an L-shaped glass tube used to illuminate the sample surface from its normal direction. As seen from the figure, a sample was fixed on the cross section of the tube, and the sample edge was covered carefully by an electronic grade wax, picene, to limit current flow to only the